

# Detection of Lateral Motion Noise and Error Ratio for Rail Wheelset Based Upon Creep

Z. A. Soomro

Mechanical Department, Quaid-e-Awam university of Engg., Science and Technology, Nawabshah,  
Sindh-Pakistan

zulfiqarali\_s@yahoo.com

**Abstract**-The knowledge about lateral motion is very crucial parameter for railway wheelset dynamics for the smooth running of railway vehicle wheels over rail track to avoid the adhesion ratio by balancing creep application. The lateral motion is caused by critical speed and high forward velocity of railway vehicle wheels. This lateral movement may be perturbed on running system on track by certain noise and disturbances, which may be necessary to be estimated to avoid accidents. In this paper, the essential dynamics of lateral motion is modeled and kalman filter is used to estimate for detection of noise to reduce disturbance and slip. The controller for Kalman estimator scheme is proposed to analyze error percentage to for controlling slippage. This slip causes the destruction of vehicle and lives. Since lateral motion is dependent upon the longitudinal speeds variations. If forward speed is higher, then the lateral speed extends due to adhesion deficiency on creepage force.

**Keywords**-Adhesion, Creep co-efficient, Lateral Speed, Kalman Filter, Error Estimation

## I. INTRODUCTION

The carter and kalker are considered as former pioneers of railway wheelset dynamics. The carter has done sufficient work on railroad vehicles while kalker paved path for dry friction procured by sliding of steel wheels on track and his concerned theories are just guide for researchers [i-ii]. The Davies has elaborated upon lateral oscillations by performing some practical on it and proved that lateral motion is affected by linear speed [iii]. The correlation between creep force and creepage is complicated for solving the rolling contact problem and effect of lateral movement for railway wheels on creepage of rail-wheel contacting surface. The concerned research in the lateral motion shows that discrimination between longitudinal creepage is smaller and possible error is lower than twenty percent. The lateral creepage on left wheel contact is more than right wheel surface as well as spin creepage of left wheel lower in lateral movement for railway wheelset. The motion of a railway wheelset move at a constant forward speed is studied that lateral motion is fixed by

flanges and the rail tracks have sinusoidal lateral deviations by wheels. The lateral motion of the wheelset can be stationary, chaotic or periodic. There are two major types of motion, [iv] one in flange contact occurs at rail and other in range of contact occurs at both rail and wheels.

The two wheels of railway wheelset are rigidly connected by an axle. The wheelset rolls on the railway contacts are considered as arc and radius of a circle. The restored force of the wheel flanges are approximated on the rail wheelset connected by strong straight springs with a dead band and without damping material. Thus lateral motion is limited by these springs without any damper. The wheelset and the axle are conceived as rigid bodies. Figure-1 shows the geometry of the railway wheelset having two degrees of freedom by movement. The rolling of a rail wheels without slipping is considered by the creep analysis. The wheels are assumed by two cones having commonly based and the rails by two circle cylinders with parallel planes [v]. The dynamics of the undisturbed rolling movement of the wheelset happens when the centre of mass moves along with a straight path. The disturbed movement describes a sinusoidal trajectory on the central mass of the wheelset.

The artificial noise does not exist on the rail-wheelset attitude at several speeds under the condition of present fluctuation noise. The lateral and yawing movements develop small amplitudes, and if the present velocity is more than the critical speed, the lateral and yawing motions arise with existing timing factor. The developing amplitude is controlled by wheel flanged contact of the wheelset to the rolling rig under the condition of the present speed. The Lateral displacements happen due to imperfections on the rail road generating uninvited movements in X, Y Z axes. The Lateral motion procures in the rail wheel contact due to their connection. These generated contact forces are discriminated as creepage forces depending upon varied creep coefficients for railroad wheelset steadiness [vi]. The creep coefficients comprise rail-wheel structure, constants and normal load.

The conventional Kalman filtering algorithm is usually application for stochastic and dynamic modeling. The dynamically model defines the nature of

modeling the errors that grow upon time while the stochastically [vii] model explains the noise of the concerned properties and new measurements of the processing to be modeled for railway wheelset.

The model was framed by using real time system for verifying validity of rail wheel contact factors for estimation of slip and sliding [xvi].

Author of this article has enumerated identification of adhesion influenced by contamination on rail track to affect the lateral phenomenon based upon creep forces associated with forward speed to cause slip [xvii].

In this paper, the railway wheelset dynamics with reference to its lateral motion is discussed to model system. The kalman filter scheme is used to estimate the noise based upon various creep co-efficient and thus error percentage is described to detect information about slippage. This kalman filter scheme is used as algorithm to differentiate the actual and estimated with their error ratio by making code on mat lab and simulink blocks as chart for implementation of mathematical relations.

## II. DYNAMICS FOR LATERAL MOTION OF RAIL-WHEELS

The attitude of a single railway wheels can be considered at a constantly moving speed  $v$  on a straight track. The mathematically model for rail wheel contain two degrees of freedom on lateral 'y' and yawing ' $\psi$ ' motions. The running direction is  $x$ , as shown in Figure 1. It is assumed that the creep force in each direction is linearly proportional to the creepage, respectively. Details of the model for the contact conditions and of the experimental derivation for the related parameters are shown in eq-5.

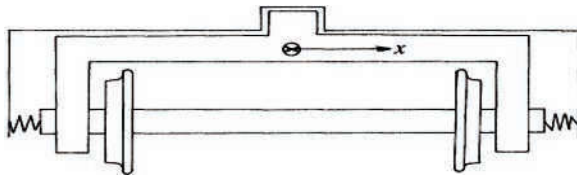


Fig.1. Railway wheelset model with lateral motion

The Creep is referred to velocity of the railway wheelset on rails. The Creep is concerned to wheels disposed laterally by left or right wheels respectively follow as under.

$$\lambda_y = \frac{\dot{y}_w - \dot{y}_v}{\dot{y}_v} \quad (1)$$

$$\text{Where } \dot{y}_v = \omega_w \cdot r = v_w \quad (2)$$

Where  $\lambda_y$  is lateral creep,  $\dot{y}$  is lateral speed and  $y_w$  is wheel speed for railway wheels as

$$v_{wR} = \omega_{wR} \cdot [r_o + \gamma (y - y_t)] \quad (3)$$

$$v_{wR} = \omega_{wR} \cdot [r_o - \gamma (y - y_t)] \quad (4)$$

Let 'F' be the horizontal force at the wheel-tread tangent to the axis, then railway wheelset is in the [viii-ix] direction for applied force divided by its distance, runs into own axis, that is "lateral creepage ( $\lambda_y$ )".

$$(\lambda_y + \psi) \cdot v = \frac{d}{dt} (y) \quad (5)$$

$$dy = \int (\lambda_{yR} + \psi) \cdot v dt \quad (6)$$

Above is lateral motion for right wheel of vehicle

$$\frac{d}{dt} (y) = (\lambda_{yL} + \psi) \cdot v \quad (7)$$

$$dy_L = \int (\lambda_{yL} + \psi) \cdot v dt \quad (8)$$

Above is lateral motion for left wheel of railway vehicle

Here ( $\lambda_{yR}$ ) and ( $\lambda_{yL}$ ) are lateral creepages of right and left wheels. If the friction coefficient is highly slip confined to a diminishing thinner zone of the rail wheel contact patch at the trailing edge. The creep forces for right and left railway wheels can be expressed using linear creep equations as under.

$$F_{yR} = f_{22} \lambda_{yR} \quad (9)$$

$$F_{yL} = f_{22} \lambda_{yL} \quad (10)$$

Where  $f_{22}$  is lateral creep force coefficients for right and left wheels respectively.

The dynamics of lateral motion is assessed by the entire creep force of railway wheelset in lateral movement way. The lateral displacement of the railway wheels is implemented by below equation.

Thus putting values of lateral creepages from equations 9 and 10 into equations 6 and 8 we get

$$dy_R = \int [(F_{yR} / f_{22}) + \psi] \cdot v dt \quad (11)$$

$$dy_L = \int [(F_{yL} / f_{22}) + \psi] \cdot v dt \quad (12)$$

Here  $\psi$  denotes the yaw motion between two wheels

## III. KALMAN FILTER CONTROL SCHEME

Kalman filter is interesting subject for extraordinary research and applications particularly in autonomous and assisted navigation fields. It is [x] combination of mathematical formulae providing an active recursive and computational sources to filter the process states to minimize the mean of the coupled errors.

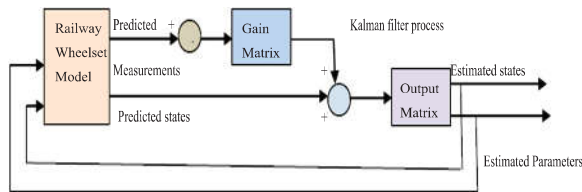


Fig. 2. Block diagram of kalman filter process for railway wheelset model

Above Fig. 2 is shown for Kalman filter processing by block diagram is conceived by author. It is observed that model is utilised to predict the systematic states and sensing inputs by measuring controlled inputs for railway system. The system study is comprised by dynamic model, provides the dynamical parts of the railway system to be filtered by kalman estimator [xi].

Kalman filters are usually depending upon the hidden Markov model system and linear algebra. The premising system modeled as a Markov chain is framed disturbed by Gaussian noises on linear operators. The railway system states can be described by vector of real numbers as Kalman filter behaves as recursive filter [xii-xiii]. It defines only the estimated states from the former time step and present measurements are required to calculate the estimation for next state of railway wheelset.

#### IV. ENVIRONMENT FOR SIMULATION

Here, the lateral motion of railway wheelset is simulated for estimating the noise through measurements by using the kalamn filter [xiv-xv] as well as detecting the error ratio for analyzing the adhesion based upon the creep. The results are enumerated as under.

##### A. Behaviour of Lateral motion of railway wheel on variation of creep co-efficient

The aforesaid lateral motion of the wheels on the rail road is displayed in the figure-3 to 5 where lateral motion of the wheels is checked by three dissimilar creep co-efficient to observe the efficiency of the railroad wheels.

The Fig. 3 reflects creep co-efficient on having value as  $10^7$ , the lateral motion of the steel wheels moves with movement of  $3.2 \times 10^{-3}$  meters at first to  $8 \times 10^{-3}$  meters within time of 0.5 seconds in zigzag way with time spans from 0.5 sec to 5 sec with increase of 0.5 seconds containing upon simulated and estimated parameters. The simulated sizes denoted by 'blue colour' moves parallel to the estimated values are marked by 'green colour' in disorder mode. Here maximum height of peak is at  $8 \times 10^{-3}$  meters in 4.4 seconds and minimum downward height of peak of curve is  $2.1 \times 10^{-3}$  meters in 4.7 seconds.

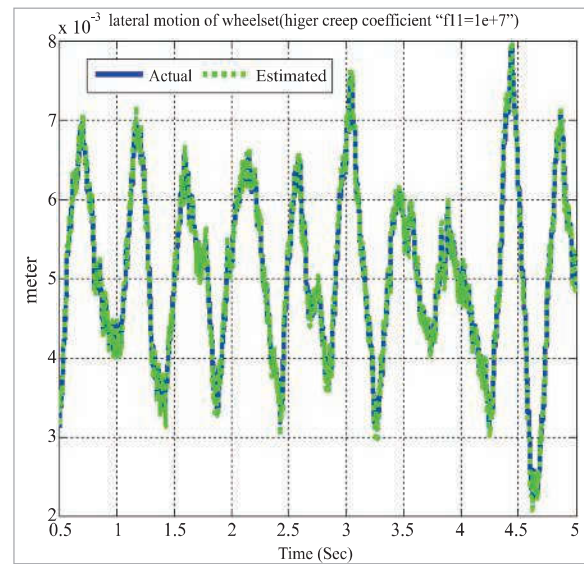


Fig. 3. lateral motion for railway wheelset on creep coefficient of  $10^7$

In Fig. 4, the creep co-efficient is projected as  $10^6$  then the lateral motion of the rail wheels vary from the 0.01 meters up to 0.03 meters for the estimated parameter in the smaller zigzag manner in time of 5 seconds. Whereas the estimated indication with tiles on time from 0.5 sec to 5 seconds with the smaller turbulence starts from -0.01 meters descending to near 11 meters. Both simulated and estimated values differ and sprint at some detachment from each other.

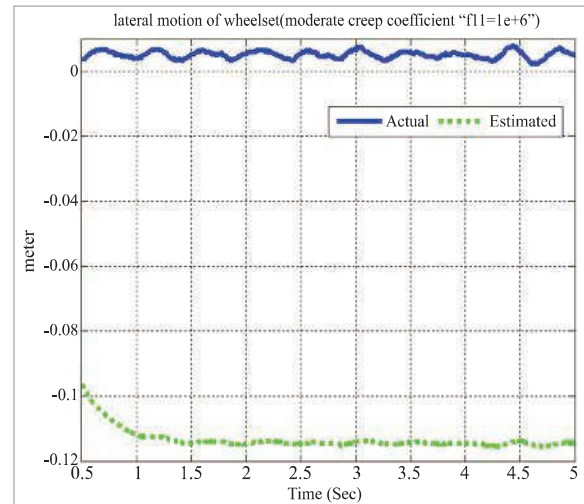


Fig. 4. Lateral motion of railway wheels on creep co-efficient of  $10^6$  for wheelset

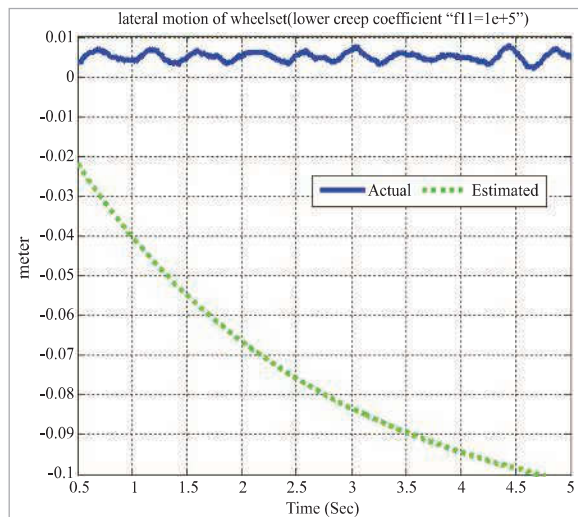


Fig. 5. Lateral motion of wheelset at creep coefficient of  $10^5$  for wheelset

In Fig. 5, the creep co-efficient is assumed as  $10^5$  then lateral motion of the wheels changes from the 0.001 meters to 0.005 meters for the estimated signal in small zigzag way in 5 seconds. While the estimated signal with flooring of time from 0.5 sec to 5 seconds with the smaller conflict starts from -0.02 meters downward lower than it to -0.11 meters with lower zigzag manner in 4.8 sec of time. Both simulated and estimated values alter and tune at a large displacement from one another.

The results obtained from both Fig. 4 and Fig. 5, resemble with each other except the image of the Fig. 3. The 1<sup>st</sup> part denotes that when the co-efficient of creep is superior, then both simulated and estimated signals partly cover each other, but when the creep co-efficient is decreased then both the simulated and estimated parameters graph lines are divorced from each other by important at smaller displacement from one another.

**B. Error judgment for lateral motion of rail wheels**

The railway vehicle dynamic signals are computed to examine the error % ratio through higher creep coefficient by blue curve and lower creep coefficient by green curve. The higher creep co-efficient is preferred as  $10^7$  and lower creep coefficient is gained as  $10^6$  for estimation of errors.

The parameters of the higher and lower creep coefficient obviously are applied to estimate the error % ratio for lateral motion of rail wheels of the vehicle in Fig. 6 as under. The black line represents higher co-efficient of creep moves in directly direction with little disturbance from zero error measured on scale. This conceives that there is none error in adhesion to cause slip denotes utmost adhesion by straight curve. Whereas low creep coefficient displayed by blue curve goes through -0.01 lower than 0 to 0.11 in arched vertical scale of error signal in upward direction while in straight way with negligible disturbances denotes

rude lack of the adhesion.

In Fig. 6, higher parameter for the error estimation is displayed by 'e1' by coefficient of creep and 'e2' is denoted by the lower error estimation based upon the creep coefficient with time in seconds horizontally plane.

The curve denoting error 'e2' by blue that line travels linearly upward shows the stability of system at 0.1 in 0.5 seconds. Then this line is converted into straight horizontal line to end at 0.108 in one second shows maximum creep.

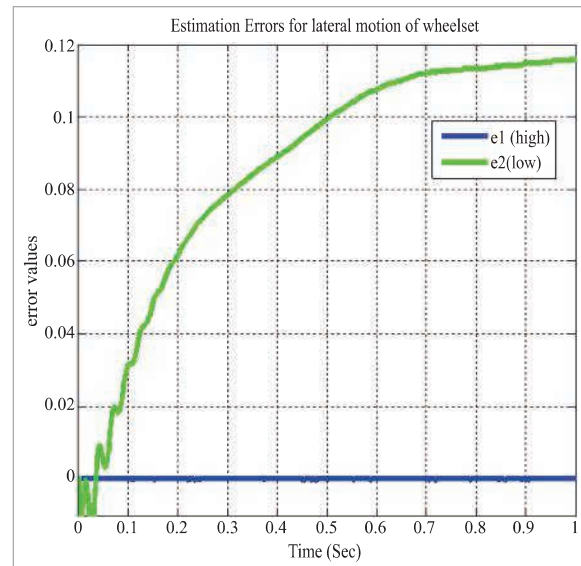


Fig. 6. Error estimation for lateral motion of wheelset

**V. CONCLUSION**

In this paper, the lateral motion of the railway wheelset is discussed and verified by its simulation results to observe their behaviour on application of three different partitions of creep co-efficient. Watching these results it can be concluded that on applying higher value of co-efficient of creep, both actual and estimated quantitative parameters travel overlapping each other in chaos zigzag manner. On average creep coefficient, both actual and estimated parameters run in zigzag way at a part distance from each other in their zones with smaller different nature. While on decreasing the ratio of creep coefficient the estimated parameter falls curved down with span of time, this conceives the idea that on decreasing creep coefficient the estimated signal provided by kalman estimator lowers away from actual line. Finally the attitude of lateral motion by error ratio is analysed to observe that creep becomes constant on higher value making slip zero, while on lower error percentage, adhesion becomes higher linearly then curves to travel in horizontal straight path.

Thus it can be concluded that lateral motion is affected by forward speed slip due to decrease in adhesion based upon creep forces to cause errors and

disturbance. So kalman filter is used to actual and estimated difference. This research on lateral analysis paves the path to develop an intelligent algorithm to control the lateral motion of railway vehicle based creep by identification of adhesion level. The error ratio also helps to monitor the adhesion information to avoid accidents due to high speed.

### NOMENCLATURE

$\omega_L, \omega_R$	Left and right wheel angular velocities
$v$	Forward Speed of Vehicle
$M_v, m_w$	Mass of vehicle and mass of wheelset
$I_R, I_L$	Moment of inertia of right wheel, left wheel
$I_w$	Yaw moment of inertia
$\Psi$	Yaw Movement
$y$	Lateral Motion
$\lambda_L, \lambda_R$	Left and right wheel Creepages
$\lambda_{Lx}, \lambda_{Rx}$	Left and right wheel creepage in longitudinal direction
$\lambda_{Ly}, \lambda_{Ry}$	Left and right wheel creepage in lateral direction
$\gamma$	Conicity of wheel
$L_g$	Half Gauge
$r_L, r_R$	Left and right wheel radius
$r_0$	Radius of each wheel when wheelset is centred
$f_{11}, f_{22}$	Longitudinal and lateral Creep force coefficients
$y_t$	Lateral Disturbance Caused by Track irregularities
$T_s, T_t$	Torsional Torque, Driving Torque
$T_L, T_R$	Tractive torque Left wheel and Right Wheel respectively

### REFERENCES

[i] F. W. Carter, "On the Action of a Locomotive Driving Wheel." Proceedings of the Royal Society of London. Series A, 1926. 112(760): p. 151-157

[ii] J. J. Kalker, "The computation of three-dimensional rolling contact with dry friction." International Journal for Numerical Methods in Engineering, 1979. 14(9): p. 1293-1307.

[iii] Davies, R.D., "some experiments on the lateral oscillation of railway vehicles". journal of the ice, 1939. 11(5): p. 224-261.

[iv] O. Polach, "Influence of wheel/rail contact geometry on the behavior of the railway vehicle at stability limit", Enoc2005, Eindhoven, Netherlands, pp 2203-2210, 7-12 August 2005.

[v] S. Y. Lee, Y. C. Cheng, "Hunting stability analysis of high-speed railway vehicle trucks on tangent tracks", Journal of Sound and Vibration, 282, pp. 881-898, 2005.

[vi] T. Sireteanu, I. Sebesan, D. Baldovin, "The influence of damping characteristic on the stabilization control of hunting motion of a railway vehicle wheelset", Proceedings of the Romanian Academy, Series A, Volume 11, Number 4//2010, pp. 355–362.

[vii] J. Choi, H. S. Ryu, C. W. Kim, J. H. Choi, "An efficient and robust contact algorithm for a compliant contact force model between bodies of complex geometry", Multibody System Dynamics 23(1)(2010)99–120.

[viii] H. Y. Cha, J. Choi, H. S. Ryu, J. H. Choi, "Stick-slip algorithm in a tangential contact force model for multi-body system dynamics", Journal of Mechanical Science and Technology 25 (7) (2011)1687–1694.

[ix] M. Fleischer, 'Reduced model identification for traction drive trains', IEEE IAS 40th annual meeting, Hong Kong, China, 2005

[x] P. Li, R. Goodall, P. Weston, C. S. Ling, C. Goodman, C. Roberts. Estimation of railway vehicle suspension parameters for condition monitoring. Control engineering practice. 2007 Jan 31;15(1):43-55.

[xi] R. U. Uzzal, W. Ahmed, S. Rakheja. Dynamic analysis of railway vehicle-track interactions due to wheel flat with a pitch-plane vehicle model. Journal of Mechanical Engineering. 2008;39(2):86-94.

[xii] M. Spiriyagin, K. S. Lee, H. H. Yoo, "Control system for maximum use of adhesive forces of a railway vehicle in a tractive mode", Mechanical Systems and Signal Processing 22, pp 709-720, 2008.

[xiii] B. R. Liang, W. S. Lin, "A new slip ratio observer and its application in electric vehicle wheel slip control, Systems", Man, and Cybernetics (SMC), 2012 IEEE International Conference on , vol., no., pp.41,46, 14-17 Oct. 2012.

[xiv] Z. A. Soomro. I. Hussain, B. S. Chowdhary. "Creep forces analysis at wheel- rail contact patch to identify adhesion level to control slip on railway track'. New Horizons, journal of IEEEP, VOL.81-82, 2014. PP.14-17.

[xv] Z. A. Soomro,. "Step Response and Estimation of Lateral and Yaw Motion Disturbance of Rail Wheel set." Journal of Engineering and Technology 5.1 (2015): 8.

[xvi] I. Hussain, "Multiple Model Based Real Time Estimation of Wheel-Rail Contact Conditions" PhD thesis. University of Salford Manchester (2012)

[xvii] Z. A. Soomro., "Development of on board Adhesion Identification System for Railway Vehicles". PhD thesis, Mehran University of Engg; & Tech; Jamshoro (2015).